Two-Dimensional Massless Dirac Fermions in Antiferromagnetic AFe_{2}As_{2} (A=Ba,Sr)

Zhi-Guo Chen (陈志国), Luyang Wang, Yu Song, Xingye Lu, Huiqian Luo, Chenglin Zhang,
Pengcheng Dai, Zhiping Yin, Kristjan Haule, and Gabriel Kotliar

Two-dimensional Massless Dirac Fermions in Antiferromagnetic $A\mathrm{Fe_2As_2}$ ($A = $ Ba, Sr)

Zhi-Guo Chen,[1, *] Luyang Wang,[2, 3] Yu Song,[4] Xingye Lu,[1] Huiqian Luo,[1] Chenglin Zhang,[4] Pengcheng Dai,[4] Zhiping Yin,[5, †] Kristjan Haule,[6, 7] and Gabriel Kotliar[6, 7]

[1]*Beijing National Laboratory for Condensed Matter Physics,*
Institute of Physics, Chinese Academy of Sciences, Beijing 100190, China
[2]*Institute for Advanced Study, Tsinghua University, Beijing 100084, China*
[3]*Sate Key Laboratory of Optoelectronic Materials and Technologies,*
School of Physics, Sun Yat-Sen University, Guangzhou 510275, China
[4]*Department of Physics and Astronomy, Rice University, Texas 77005, USA*
[5]*Center of Advanced Quantum Studies and Department of Physics,*
Beijing Normal University, Beijing 100875, China
[6]*Department of Physics and Astronomy, Rutgers University, New Jersey 08854, USA*
[7]*DMFT-MatDeLab Center, Upton, New York 11973, USA*

We report infrared studies of $A\mathrm{Fe_2As_2}$ ($A = $ Ba, Sr), two representative parent compounds of iron-arsenide superconductors, at magnetic fields (B) up to 17.5 T. Optical transitions between Landau levels (LLs) were observed in the antiferromagnetic states of these two parent compounds. Our observation of a $\sqrt{B}$ dependence of the LL transition energies, the zero-energy intercepts at $B = 0$ T under the linear extrapolations of the transition energies and the energy ratio (~ 2.4) between the observed LL transitions, combined with the linear band dispersions in two-dimensional (2D) momentum space obtained by theoretical calculations, demonstrates the existence of massless Dirac fermions in antiferromagnetic $\mathrm{BaFe_2As_2}$. More importantly, the observed dominance of the zeroth-LL-related absorption features and the calculated bands with extremely weak dispersions along the momentum direction k_z indicate that massless Dirac fermions in $\mathrm{BaFe_2As_2}$ are *2D*. Furthermore, we find that the total substitution of the barium atoms in $\mathrm{BaFe_2As_2}$ by strontium atoms not only maintains 2D massless Dirac fermions in this system, but also enhances their Fermi velocity, which supports that the Dirac points in iron-arsenide parent compounds are topologically protected.

In condensed matters, massless Dirac fermions (MDF), which represent a type of quasi-particles with linear energy-momentum dispersions, provide a cornerstone for various quantum phenomena, such as novel quantum Hall effect[1–3], Klein tunnelling[4] and giant linear magneto-resistance[5]. Due to their crucial role in diverse quantum phenomena, searching for MDF in new systems is one of the most active research areas in condensed matter science. Generally, massless Dirac fermions with their valence and conduction band touching at a degenerate point (i.e. Dirac point) are protected by symmetries in solids[6–10]. However, the formation of magnetic order is always accompanied with time-reversal symmetry breaking and sometimes followed by crystalline symmetry lowering. Therefore, it is a challenge to achieve MDF in magnetic ground states of solid-state electronic systems [11, 12]. Moreover, two-dimensional (2D) MDF, which were realized in 2D materials and on the surfaces of three-dimensional (3D) topological insulators [1–3, 13–17], have rarely been observed in the bulk of 3D crystals [11]. The discovery of iron-arsenide superconductors not only brings people a new class of unconventional superconductivity [18], but also sheds light on seeking 2D MDF in magnetic compounds[19, 20].

The parent compounds of iron-arsenide superconductors (PCIS) exhibit collinear antiferromagnetic (AFM) order at low temperature (T)[21, 22]. After the AFM phase transition, the paramagnetic Brillouin zone of PCIS would be folded along the AFM wave vector con-

necting the hole-type Fermi surfaces (FSs) surrounding the Γ point and the electron-type FSs at the M point, which leads to the intersection between the electron- and hole-bands and results in the bandgap opening at the band crossing points near Fermi energy (E_F) [23–27]. However, theoretical studies suggest that for PCIS, some band crossing points are *topologically* protected by (i) the collinear AFM order, (ii) inversion symmetry and (iii) a combination of time-reversal and spin-reversal symmetry [19, 20]. Furthermore, angle-resolved photoemission spectroscopy (ARPES) measurements of $\mathrm{BaFe_2As_2}$ show linear band dispersions within k_x-k_y plane below E_F [28]. Therefore, massless fermions, which are characterized by band-degeneracy points and linear energy-momentum dispersions, are expected to exist in the AFM state of $\mathrm{BaFe_2As_2}$ [19, 20, 25, 28–34]. There are three types of massless fermions, including MDF, massless Kane fermions and Weyl fermions [35–42]. Therein, massless Kane fermions and Weyl fermions are characterized by a heavy-hole valence band around the band-degeneracy point and pairs of degenerate nodes with opposite chirality, respectively[35–39], while in PCIS, the heavy-hole valence band is absent and the degenerate nodes have the same chirality[19, 20, 28, 31], which preclude the association of the observed linear band dispersions by ARPES with massless Kane fermions and Weyl fermions. Therefore, massless fermions in PCIS were suggested to be MDF [19, 20, 25, 28–34]. However, whether MDF in PCIS are 2D or 3D remains unclear. Further

studies are needed to clarify the dimensionality of MDF in PCIS. Besides, in order to verify whether the degenerate points of PCIS are topologically protected, it is important to experimentally test the robustness of the band crossing points in this system. Experimental investigations of the optical transitions between Landau levels (LLs), combined with band-structure calculations, can provide strong evidence for identifying the nature of MDF in PCIS.

Infrared spectroscopy is a bulk-sensitive experimental technique for investigating low-energy excitations of a material. Here, to study the LL transitions in PCIS, we measured the infrared reflectance spectra $R(B)$ of $A\text{Fe}_2\text{As}_2$ (A = Ba, Sr) single crystals in their AFM states ($T \sim 4.5$ K) with the magnetic field applied along the wave vector of the incident light and the crystalline c-axis (i.e. Faraday geometry) [43]. Landau-level-transition features are present in the relative reflectance spectra $R(B)/R(B_0 = 0 \text{ T})$ of these two PCIS. Our observation of a $\sqrt{B}$ dependence of the LL transition energies, the zero-energy intercepts at $B = 0$ T under the linear extrapolations of the transition energies, the energy ratio (~ 2.4) between the two measured LL transitions and the dominant absorption features of the zeroth-LL-related transitions, combined with the linear band dispersions in 2D momentum space calculated using the density functional theory and dynamical mean field theory (DFT+DMFT), indicates *2D* MDF in AFM BaFe_2As_2. Moreover, to test the robustness of MDF in this system, we completely replaced the barium atoms in BaFe_2As_2 with strontium atoms, causing a distortion of the crystal structure [44]. Our investigations show that 2D MDF not only exist in SrFe_2As_2, but also have larger effective Fermi velocity after substituting the barium atoms, which provides evidence for the topologically protected Dirac points in PCIS.

Figure 1(a) depicts the false-color map of the $R(B)/R(B_0 = 0 \text{ T})$ spectra of BaFe_2As_2 as a function of magnetic field and energy. As displayed in Fig. 1(b), peak-like features are present in $R(B)/R(B_0 = 0 \text{ T})$ and systematically shift to higher energies as the magnetic field increases. A fundamental question is what these peak-like features arise from. Largely due to the strong (next) nearest neighbor exchange coupling[45], an ultra-high magnetic field ($B > 500$ T) along the crystalline c-axis is estimated to destroy the low-temperature collinear AFM order in PCIS[46]. The applied magnetic field ($B \leq 17.5$ T) here is therefore too low to dramatically change the AFM order at $T \sim 4.5$ K. In addition, the AFM-order-related spectral-weight-transfer in the reflectance spectra of BaFe_2As_2 takes place in the energy range up to about 250 meV[23–27], which is much wider than that observed in Fig. 1 (b) (~ 55 meV). Based on the applied magnetic field and energy range of the spectral-weight-transfer here, the observed peak-like features are unlikely to originate from the magnetic-field-
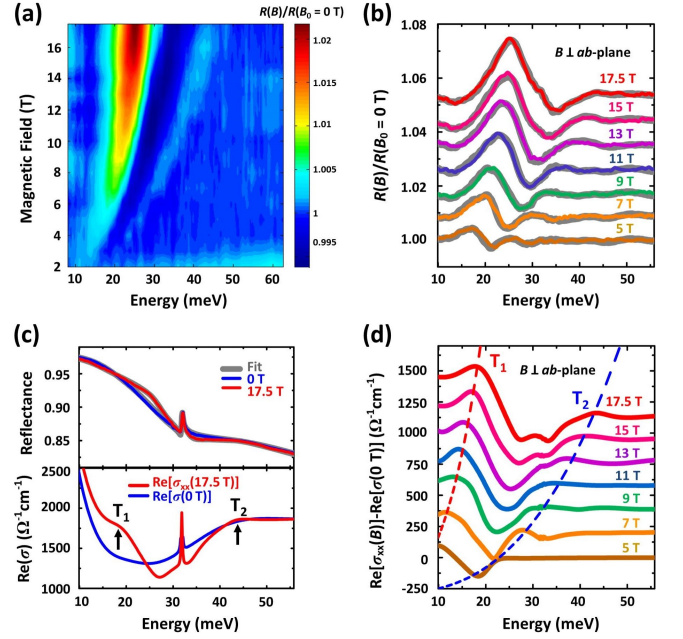

FIG. 1: Magneto-optical response of BaFe_2As_2. (a) False-color map of the $R(B)/R(B_0 = 0 \text{ T})$ spectra. See the false-color map plotted as a function of $\sqrt{B}$ and energy in Supplementary Fig. 4. (b) Several representative $R(B)/R(B_0 = 0 \text{ T})$ spectra and their fitting results (grey curves). The $R(B)/R(B_0 = 0 \text{ T})$ spectra up to 120 meV are shown in Supplementary Fig. 5. (c) Upper panel: the reflectance spectra at $B = 0$ T and $B = 17.5$ T, and their fitting results. Lower panel: the real part of $\sigma_{xx}(B, \omega)$ at $B = 17.5$ T and $\sigma(0 \text{ T}, \omega)$. The two black arrows in $\text{Re}[\sigma_{xx}(B = 17.5 \text{ T}, \omega)]$ indicate two additional peaks, T_1 and T_2. (d) Relative real part of the optical conductivity. The blue and red dashed lines are guides to eyes. Except T_1 and T_2, another peak emerges around 31 meV in (b) and (d) at $B > 13$ T (see its possible origin in Supplementary Section 2, which includes Refs. [52–54]). The spectra in (b) and (d) are displaced from one another by 0.09 and 240 (Ω^{-1} cm^{-1}) for clarity.

induced change in the AFM order. Besides, structural twins form in the orthorhombic crystal of BaFe_2As_2 below the AFM phase transition temperature[47, 48]. The magnetic field applied along the orthorhombic a- or b-axis can be used for partially detwinning BaFe_2As_2 single crystals[49]. Here, the magnetic field applied perpendicular to the ab-plane cannot detwin the single crystals, so the observed peak features in Fig. 1(b) are irrelevant with the detwinning[50]. Given the magnetic-field-dependent energy positions, the peak features should arise from the optical absorption of the LL transitions in BaFe_2As_2.

To identify the nature of the LL transitions in BaFe_2As_2, we need to extract the absorption energies of the LL transitions from the measured reflectance spectra. Using the magneto-optical model to fit the absolute reflectance $R(B)$ at a fixed magnetic field[51] (see the grey curves in Fig. 1(b) and the upper panel of Fig. 1(c)), we
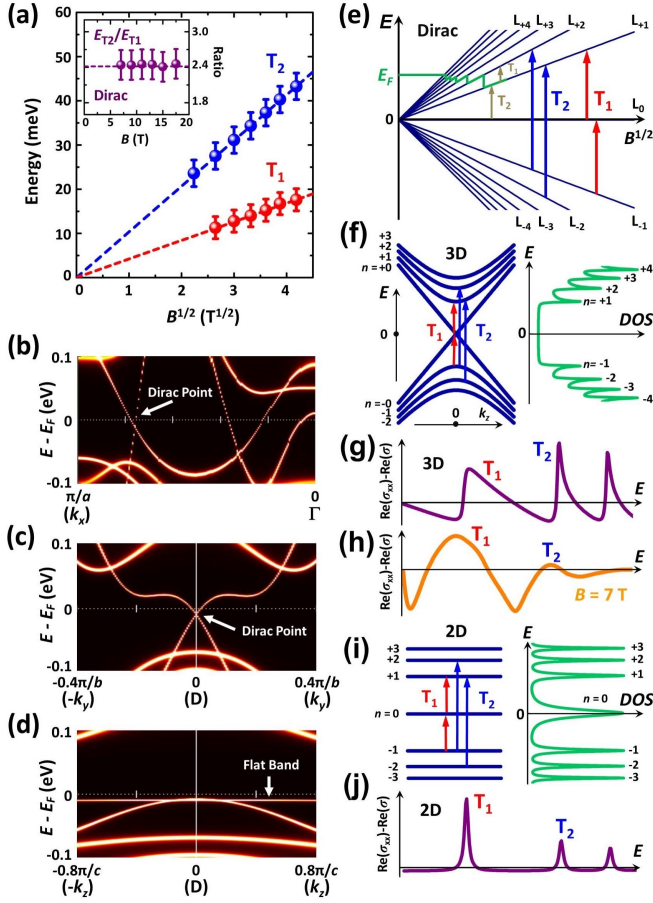
FIG. 2: Landau level transitions and band dispersions of BaFe$_2$As$_2$ in the AFM state. (a) Observed LL transitions, T$_1$ and T$_2$, in an E-$\sqrt{B}$ plot. The inset shows the energy ratio of T$_1$ and T$_2$ as a function of B. The purple dashed line shows the theoretical energy ratio based on MDF model. (b-d) Calculated band dispersions along k_x, k_y and k_z near E_F. The flat band in (d) represents the dispersion of MDF along k_z. In the AFM Brillouin zone of AFe$_2$As$_2$ (A = Ba, Sr), -$\pi/a \leq k_x \leq \pi/a$, -$\pi/b \leq k_y \leq \pi/b$ and -$2\pi/c \leq k_z \leq 2\pi/c$, where a, b and c are the lattice constants. (e) Schematic of the LL transitions of 2D MDF in BaFe$_2$As$_2$. The green lines show the magnetic field dependence of the assumed E_F. (f) Left panel: LLs of 3D MDF. Right panel: DOS of 3D MDF. (g) Calculated relative real part of the optical conductivity of 3D MDF based on Eq. (15) of Ref. [61]. (h) Re[$\sigma_{xx}(B)$] − Re[$\sigma(0$ T)] of BaFe$_2$As$_2$ at $B = 7$ T. (i) Left panel: LLs of 2D MDF. Right panel: Lorentz-shaped DOS of 2D MDF. (j) Calculated Re[$\sigma_{xx}(B)$] − Re[$\sigma(0$ T)] of 2D MDF based on Eq. (23) of Ref [62]. When calculating the spectra in (g) and (j), we replaced the Kronecker delta functions in Eq. (15) of Ref. [61] and Eq. (23) of Ref [62] by the Lorentzian functions with non-zero scattering rates.

obtained the dielectric function tensor $\varepsilon_\pm(B, \omega)$ for the right and left circularly polarized light and then got the real part of the diagonal optical conductivity Re[$\sigma_{xx}(B, \omega)$] [43]. Figure 1(c) shows the obtained Re[$\sigma_{xx}(B = 17.5$ T, $\omega)$] of BaFe$_2$As$_2$. Compared with the Re[$\sigma(B =$

0 T, $\omega)$] of BaFe$_2$As$_2$ in the AFM state, Re[$\sigma_{xx}(B = 17.5$ T, $\omega)$] has two additional peak-like features: T$_1$ and T$_2$, which are better resolved in Re[$\sigma_{xx}(B = 17.5$ T, $\omega)$] − Re[$\sigma(B = 0$ T, $\omega)$] (see Fig. 1(d)). These two peak-like features, which move towards higher energies with increasing the magnetic field, correspond to the absorption modes of the LL transitions. Following the definition in the magneto-optical study of BiTeI[55], we assign the peak positions in Re[$\sigma_{xx}(B = 17.5$ T, $\omega)$] − Re[$\sigma(B = 0$ T, $\omega)$] to the LL transition energies.

We plotted the T$_1$ and T$_2$ energies as a function of $\sqrt{B}$ in Fig. 2(a). Both T$_1$ and T$_2$ energies exhibit a linear dependence on $\sqrt{B}$ and the zero intercepts at $B = 0$ T under linear extrapolations. Moreover, the T$_2$ and T$_1$ energies scale as 2.4 : 1 (see the inset of Fig. 2(a)). The $\sqrt{B}$-dependence of the LL transition energies and the zero-energy intercepts at $B = 0$ T are two signatures of MDF[55–58]. To identify the dimensionality of MDF in BaFe$_2$As$_2$, we performed DFT+DMFT calculations [43, 59, 60]. In Fig. 2(b)-(d), our calculations show that in the AFM state, the band dispersions near E_F are linear along k_x and k_y directions, but extremely weak along k_z direction, which theoretically suggests 2D MDF in BaFe$_2$As$_2$. According to the effective Hamiltonian describing 2D MDF in PCIS[20], we can obtain (i) the LL energy spectrum without considering Zeeman effects [43]:

$$E_n^{2D} = \text{sgn}(n)\sqrt{2e\hbar v_F^2 |n| B} \tag{1}$$

where the integer n is LL index, sgn(n) is the sign function, v_F is the effective Fermi velocity of LLs, e is the elementary charge and $\hbar$ is Planck's constant divided by 2π, and (ii) the selection rule for the allowed optical transitions from LL$_n$ to LL$_{n'}$ [43]:

$$\Delta n = |n| - |n'| = \pm 1. \tag{2}$$

According to Eq. (1), the energies of the allowed optical transitions from LL$_n$ to LL$_{n'}$ are given by:

$$E_{n \to n'}^{2D} = \text{sgn}(n')\sqrt{2e\hbar v_F^2 |n'| B} - \text{sgn}(n)\sqrt{2e\hbar v_F^2 |n| B} \tag{3}$$

Indeed, the LL transition energies of 2D MDF exhibit a linear dependence on $\sqrt{B}$ and converge to zero at $B = 0$ T. More importantly, equation (2) and (3) indicate that two groups of optical transitions between the LLs of 2D MDF have the energy ratios which are quite close to that between T$_1$ and T$_2$: (i) $(\sqrt{2}-1) : 1 \approx 1 : 2.414$ for the LL transitions, LL$_{-2} \to$ LL$_{-1}$ and LL$_{-1} \to$ LL$_0$ (or LL$_{+1} \to$ LL$_{+2}$ and LL$_0 \to$ LL$_{+1}$), and (ii) $1 : (1+\sqrt{2}) \approx 1 : 2.414$ for the LL transitions, LL$_{-1} \to$ LL$_0$ and LL$_{-1} \to$ LL$_{+2}$ (or LL$_0 \to$ LL$_{+1}$ and LL$_{-2} \to$ LL$_{+1}$). For case (i) (see the two grey arrows in Fig. 2(e)), we can expect: (1) $v_F \approx 2.85 \times 10^5$ m/s, calculated based on Eq. (3), (2) E_F (see the green line in Fig. 2(e)) should be pinned on LL$_{+1}$ (or LL$_{-1}$), even at $B = 17.5$ T. (If E_F was pinned on the LLs higher than LL$_{+1}$ (or LL$_{-1}$), e.g. LL$_{+2}$ (or

LL$_{-2}$), LL$_{+1}$ (or LL$_{-1}$) should be fully occupied (or depleted). According to Pauli exclusion principle, LL$_0 \rightarrow$ LL$_{+1}$ (or LL$_{-1} \rightarrow$ LL$_0$) would be blocked. If E_F was pinned on LL$_0$, LL$_{-1}$ (or LL$_{+1}$) should be fully occupied (or depleted). Then LL$_{-2} \rightarrow$ LL$_{-1}$ (or LL$_{+1} \rightarrow$ LL$_{+2}$) would be blocked. Thus, if E_F was not pinned on LL$_{+1}$ or LL$_{-1}$, one type of the LL transitions in case (i) would not occur. See Supplementary Fig. 6) and (3) the spectral weight of the assumed LL transition T$_1$ should decrease as the magnetic field increases, since LL$_{+1}$ (or LL$_{-1}$) is depopulated by the magnetic field[56]. In contrast, T$_1$ in Fig. 1(b) and (d) becomes more dominant with the enhancement of the magnetic field. Besides, based on the above v_F and equation (1), the corresponding E_F in BaFe$_2$As$_2$ is at least 179 meV, which is much higher than the measured Fermi energy of $\sim$ 1 meV by ARPES[28]. Thus, T$_1$ and T$_2$ should not come from the LL transitions in case (i). Case (ii) (see the red and blue arrows in Fig. 2(e)) means that the system has been in the quantum limit at $B \leq 5$ T , which is consistent with the low E_F measured by ARPES[28]. By fitting the $\sqrt{B}$-dependence of the energies of T$_1$ and T$_2$ in case (ii) based on Eq. (3), we deduced $v_F \approx 1.18 \times 10^5$ m/s, which is comparable to the values reported by ARPES and transport measurements[28, 30]. Therefore, T$_1$ and T$_2$ arise from the LL transitions, LL$_{-1} \rightarrow$ LL$_0$ and LL$_{-1} \rightarrow$ LL$_{+2}$ (or LL$_0 \rightarrow$ LL$_{+1}$ and LL$_{-2} \rightarrow$ LL$_{+1}$), respectively.

When $E_F \sim 0$, 3D Dirac semimetals also have a $\sqrt{B}$ dependence of the LL transition energies at low magnetic fields [37]. Further evidence is required to determine whether MDF in BaFe$_2$As$_2$ are 2D or 3D. The left panel of Fig. 2(f) shows that at magnetic fields, the band dispersions of 3D MDF are transformed into a series of one-dimensional LLs (or Landau bands), which disperse with the momentum component along the field direction. The LL spectrum of 3D MDF has the form:

$$E_n^{3D} = \pm \delta_{n,0} v_z \hbar k_z + \mathrm{sgn}(n)\sqrt{2e\hbar v_F^2 |n|B + (v_z \hbar k_z)^2} \ (4)$$

where $\delta_{n,0}$ is the Kronecker delta function, k_z is the momentum along z-axis, v_z is the Fermi velocity along k_z direction. In the right panel of Fig. 2(f), the zeroth LLs of 3D MDF disperse linearly with k_z and thus do not have a singularity of the density of states (DOS), while the other LLs have the singularities of DOS at $k_z = 0$ [37]. Since optical absorptions are determined by the joint DOS of the initial and final state, figure 2(g), which was obtained by the theoretical calculations based on the model of the optical conductivity of 3D linear band dispersions (see Eq. (15) of Ref. [61]), shows that the peak feature (i.e. T$_1$) of the zeroth-LL-related transition LL$_{-1} \rightarrow$ LL$_{\pm 0}$ (or LL$_{\pm 0} \rightarrow$ LL$_{+1}$) in Re$[\sigma_{xx}(B)] -$ Re$[\sigma(0$ T$)]$ is *weaker* than that (i.e. T$_2$) of the LL transition LL$_{-1} \rightarrow$ LL$_{+2}$ (or LL$_{-2} \rightarrow$ LL$_{+1}$). In contrast, the Re$[\sigma_{xx}(B = 7$ T$)] -$ Re$[\sigma(0$ T$)]$ of BaFe$_2$As$_2$ in Fig. 2(h) show that its peak feature (i.e. T$_1$) of the zeroth-LL-related transition LL$_{-1} \rightarrow$ LL$_0$ (or LL$_0 \rightarrow$ LL$_{+1}$) is much stronger
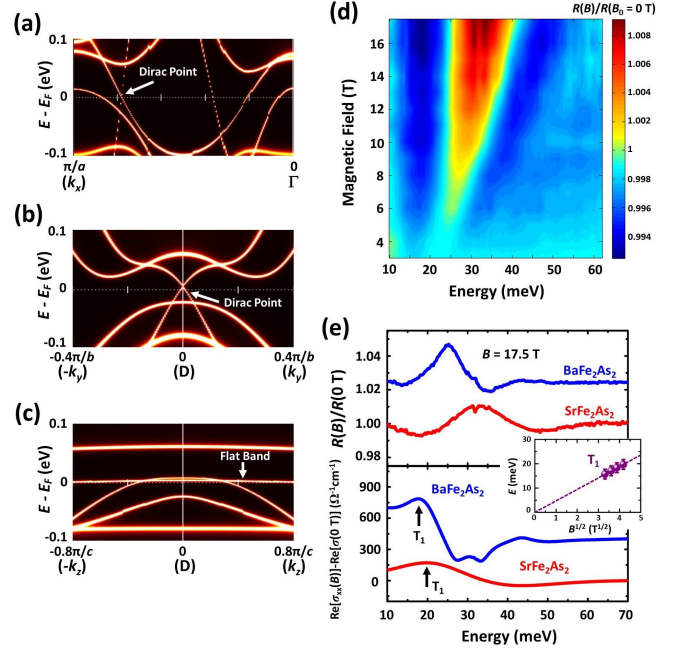

FIG. 3: Magneto-optical response and band dispersions of SrFe$_2$As$_2$ in the AFM state. (a-c) Energy-momentum dispersions of MDF in SrFe$_2$As$_2$ along k_x, k_y and k_z. The flat band in (c) shows the dispersion of MDF along k_z. (d) False-color map of the $R(B)/R(B_0 = 0$ T$)$ spectra of SrFe$_2$As$_2$ as a function of B and E. (e) Relative reflectance (upper panel) and relative optical conductivity (lower panel) spectra of BaFe$_2$As$_2$ and SrFe$_2$As$_2$ at $B = 17.5$ T. The inset shows the $\sqrt{B}$-dependence of the observed T$_1$ transition energy. The spectra of BaFe$_2$As$_2$ in (e) are displaced from those of SrFe$_2$As$_2$ by 0.023 and 412 (Ω^{-1} cm^{-1}) for clarity.

than its T$_2$ feature, indicating that MDF in BaFe$_2$As$_2$ should *not* be 3D. On the contrary to the zeroth LLs of 3D MDF, the LL$_0$ of 2D MDF has a singularity of DOS at zero energy (see Fig. 2(i)). Thus, in Fig. 2(j), the theoretical calculations based on Eq. (23) of Ref. [62] reveal that the peak feature (i.e. T$_1$) of the LL$_0$-related transition of 2D MDF is stronger than the T$_2$ feature of 2D MDF, which is consistent with our magneto-infrared results of BaFe$_2$As$_2$. The relative intensities of T$_1$ and T$_2$, combined with the calculated band dispersions along k_x, k_y and k_z directions, indicate 2D MDF in BaFe$_2$As$_2$.

To test the robustness of the Dirac points in PCIS, we completely replaced the barium atoms in BaFe$_2$As$_2$ by strontium atoms. The element replacement causes a crystal distortion, but (1) the AFM order still exists, and (2) inversion symmetry and the combination of time-reversal and spin-reversal symmetry are not broken[44]. In Fig. 3(a)-(c), our DFT+DMFT calculations show the linear band dispersions along k_x and k_y directions and the quite weak dispersions along k_z direction, indicating 2D MDF in SrFe$_2$As$_2$. We further performed magneto-reflectance measurements of SrFe$_2$As$_2$ single crystals at $T \sim 4.5$ K in Faraday geometry (see Fig. 3(d)). In Fig. 3(e), the peak

features in the relative reflectance and relative optical conductivity spectra of $SrFe_2As_2$ at $B = 17.5$ T, which arise from the optical transition $LL_{-1} \rightarrow LL_0$ (or $LL_0 \rightarrow LL_{+1}$), appear at higher energies than those of $BaFe_2As_2$, implying a larger effective Fermi velocity of the LLs in $SrFe_2As_2$ (see the spectra at some other magnetic fields in Supplementary Fig. 7). For $SrFe_2As_2$, in the inset of Fig. 3(e), the energy positions of the peaks in its relative optical conductivity spectra show a linear dependence on $\sqrt{B}$ and converge to zero at zero-field, consistent with the DFT+DMFT calculation results about 2D MDF. Fitting the $\sqrt{B}$-dependence of the peak features of $SrFe_2As_2$ yields $v_F \approx 1.30 \times 10^5$ m/s, which is indeed larger than that of $BaFe_2As_2$. Our infrared study, combined with the DFT+DMFT calculations, manifests that the substitution of the barium atoms in $BaFe_2As_2$ by strontium atoms not only maintains 2D MDF, but also enhances their effective Fermi velocity, providing evidence for the topologically protected Dirac points in PCIS.

In summary, our observation of the $\sqrt{B}$-dependence of the LL transition energies, the zero-energy intercept at $B = 0$ T under linear extrapolations of the transition energies, the energy ratio (~ 2.4) and the dominant absorption features of the zeroth-LL-related transitions, together with the linear band dispersions in 2D momentum space obtained by DFT+DMFT calculations, not only demonstrates the existence of 2D MDF, but also provides support for the topological protection of the Dirac points in the AFM states of two iron-arsenide parent compounds—$BaFe_2As_2$ and $SrFe_2As_2$.

 Electronic address: zgchen@iphy.ac.cn
[†] Electronic address: yinzhiping@bnu.edu.cn

[1] K. S. Novoselov, A. K. Geim, S. V. Morozov, D. Jiang, Y. Zhang, S. V. Dubonos, I. V. Grigorieva, and A. A. Firsov, Science **306**, 666-669 (2004).

[2] K. S. Novoselov, A. K. Geim, S. V. Morozov, D. Jiang, M. I. Katsnelson, I. V. Grigorieva, S. V. Dubonos, and A. A. Firsov, Nature **438**, 197-200 (2005).

[3] Yuanbo Zhang, Yan-Wen Tan, Horst L. Stormer, and Philip Kim, Nature **438**, 201 (2005).

[4] C. W. J. Beenakker, Rev. Mod. phys. **80**, 1337 (2008).

[5] Tian Liang, Quinn Gibson, Mazhar N. Ali, Minhao Liu, R. J. Cava, and N. P. Ong, Nat. Mater. **14**, 280-284 (2015).

[6] M. Z. Hasan, and C. L. Kane, Rev. Mod. Phys. **82**, 3045 (2010).

[7] Xiao-Liang Qi, and Shou-Cheng Zhang, Rev. Mod. Phys. **83**, 1057 (2011).

[8] Z. K. Liu, B. Zhou, Y. Zhang, Z. J. Wang, H. M. Weng, D. Prabhakaran, S.-K. Mo, Z. X. Shen, Z. Fang, X. Dai, Z. Hussain, and Y. L. Chen, Science **343**, 864-867 (2014).

[9] Madhab Neupane, Su-Yang Xu, Raman Sankar, Nasser Alidoust, Guang Bian, Chang Liu, Ilya Belopolski, Tay-Rong Chang, Horng-Tay Jeng, Hsin Lin, Arun Bansil, Fangcheng Chou, and M. Zahid Hasan, Nat. Commun. **5**, 3786 (2014).

[10] Sergey Borisenko, Quinn Gibson, Danil Evtushinsky, Volodymyr Zabolotnyy, Bernd Büchner, and Robert J. Cava, Phys. Rev. Lett. **113**, 027603 (2014).

[11] Joonbum Park, G. Lee, F. Wolff-Fabris, Y. Y. Koh, M. J. Eom, Y. K. Kim, M. A. Farhan, Y. J. Jo, C. Kim, J. H. Shim, and J. S. Kim, Phys. Rev. Lett. **107**, 126402 (2011).

[12] Peizhe Tang, Quan Zhou, Gang Xu, and Shou-Cheng Zhang, Nat. Phys. **12**, 1100 (2016).

[13] Ya Feng, Defa Liu, Baojie Feng, Xu Liua, Lin Zhao, Zhuojin Xie, Yan Liu, Aiji Liang, Cheng Hu, Yong Hu, Shaolong He, Guodong Liu, Jun Zhang, Chuangtian Chen, Zuyan Xu, Lan Chen, Kehui Wu, Yu-Tzu Liu, Hsin Lin, Zhi-Quan Huang, Chia-Hsiu Hsu, Feng-Chuan Chuang, Arun Bansil, and X. J. Zhou, Proc. Natl. Acad. Sci. USA **113**, 14656-14661 (2016).

[14] D. Hsieh, D. Qian, L. Wray, Y. Xia, Y. S. Hor, R. J. Cava, and M. Z. Hasan, Nature **452**, 970 (2008).

[15] Y. L. Chen, J. G. Analytis, J.-H. Chu, Z. K. Liu, S.-K. Mo, X. L. Qi, H. J. Zhang, D. H. Lu, X. Dai, Z. Fang, S. C. Zhang, I. R. Fisher, Z. Hussain, and Z.-X. Shen, Science **325**, 178 (2009).

[16] Peng Cheng, Canli Song, Tong Zhang, Yanyi Zhang, Yilin Wang, Jin-Feng Jia, Jing Wang, Yayu Wang, Bang-Fen Zhu, Xi Chen, Xucun Ma, Ke He, Lili Wang, Xi Dai, Zhong Fang, Xincheng Xie, Xiao-Liang Qi, Chao-Xing Liu, Shou-Cheng Zhang, and Qi-Kun Xue, Phys. Rev. Lett. **105**, 076801 (2010).

[17] T. Hanaguri, K. Igarashi, M. Kawamura, H. Takagi, and T. Sasagawa, Phys. Rev. B **82**, 081305(R) (2010).

[18] Yoichi Kamihara, Takumi Watanabe, Masahiro Hirano,

and Hideo Hosono, J. Am. Chem. Soc. **130**, 3296-3297 (2008).

[19] Ying Ran, Fa Wang, Hui Zhai, Ashvin Vishwanath, and Dung-Hai Lee, Phys. Rev. B **79**, 014505 (2009).

[20] Takao Morinari, Eiji Kaneshita, and Takami Tohyama, Phys. Rev. Lett. **105**, 037203 (2010).

[21] Q. Huang, Y. Qiu, Wei Bao, M. A. Green, J. W. Lynn, Y. C. Gasparovic, T. Wu, G. Wu, and X. H. Chen, Phys. Rev. Lett. **101**, 257003 (2008).

[22] Jun Zhao, W. Ratcliff, II, J. W. Lynn, G. F. Chen, J. L. Luo, N. L. Wang, Jiangping Hu, and Pengcheng Dai, Phys. Rev. B **78**, 140504(R) (2008).

[23] W. Z. Hu, J. Dong, G. Li, Z. Li, P. Zheng, G. F. Chen, J. L. Luo, and N. L. Wang, Phys. Rev. Lett. **105**, 257005 (2008).

[24] Z. G. Chen, T. Dong, R. H. Ruan, B. F. Hu, B. Cheng, W. Z. Hu, P. Zheng, Z. Fang, X. Dai, and N. L. Wang, Phys. Rev. Lett. **105**, 097003 (2010).

[25] M. Nakajima, T. Liang, S. Ishida, Y. Tomioka, K. Kihou, C. H. Lee, A. Iyo, H. Eisaki, T. Kakeshita, T. Ito, and S. Uchida, Proc. Natl. Acad. Sci. USA **108**, 12238-12242 (2011).

[26] S. J. Moon, A. A. Schafgans, S. Kasahara, T. Shibauchi, T. Terashima, Y. Matsuda, M. A. Tanatar, R. Prozorov, A. Thaler, P. C. Canfield, A. S. Sefat, D. Mandrus, and D. N. Basov, Phys. Rev. Lett. **109**, 027006 (2012).

[27] Y. M. Dai, Ana Akrap, S. L. Bud'ko, P. C. Canfield, and C. C. Homes, Phys. Rev. B **94**, 195142 (2016).

[28] P. Richard, K. Nakayama, T. Sato, M. Neupane, Y.-M. Xu, J. H. Bowen, G. F. Chen, J. L. Luo, N. L. Wang, X. Dai, Z. Fang, H. Ding, and T. Takahashi, Phys. Rev. Lett. **104**, 137001 (2010).

[29] N. Harrison, and S. E. Sebastian, Phys. Rev. B **80**, 224512 (2009).

[30] Khuong K. Huynh, Yoichi Tanabe, and Katsumi Tanigaki, Phys. Rev. Lett. **106**, 217004 (2011).

[31] Taichi Terashima, Nobuyuki Kurita, Megumi Tomita, Kunihiro Kihou, Chul-Ho Lee, Yasuhide Tomioka, Toshimitsu Ito, Akira Iyo, Hiroshi Eisaki, Tian Liang, Masamichi Nakajima, Shigeyuki Ishida, Shin-ichi Uchida, Hisatomo Harima, and Shinya Uji, Phys. Rev. Lett. **107**, 176402 (2011).

[32] Marcin Matusiak, Zbigniew Bukowski, and Janusz Karpinski, Phys. Rev. B **83**, 224505 (2011).

[33] Shunji Sugai, Yuki Mizuno, Ryoutarou Watanabe, Takahiko Kawaguchi, Koshi Takenaka, Hiroshi Ikuta, Yasumasa Takayanagi, Naoki Hayamizu, and Yasuhiro Sone, J. Phys. Soc. Jpn. **81**, 024718 (2012).

[34] Yoshinori Imai, Fuyuki Nabeshima, Daisuke Nakamura, Takayoshi Katase, Hidenori Hiramatsu, Hideo Hosono, and Atsutaka Maeda, J. Phys. Soc. Jpn. **82**, 043709 (2013).

[35] M. Orlita, D. M. Basko, M. S. Zholudev, F. Teppe, W. Knap, V. I. Gavrilenko, N. N. Mikhailov, S. A. Dvoretskii, P. Neugebauer, C. Faugeras, A-L. Barra, G. Martinez, and M. Potemski, Nat. Phys. **10**, 233 (2014).

[36] F. Teppe, M. Marcinkiewicz, S. S. Krishtopenko, S. Ruffenach, C. Consejo, A. M. Kadykov, W. Desrat, D. But, W. Knap, J. Ludwig, S. Moon, D. Smirnov, M. Orlita, Z. Jiang, S. V. Morozov, V.I. Gavrilenko, N. N. Mikhailov, and S. A. Dvoretskii, Nat. Commun. **7**, 12576 (2016).

[37] A. Akrap, M. Hakl, S. Tchoumakov, I. Crassee, J. Kuba, M. O. Goerbig, C. C. Homes, O. Caha, J. Novák, F. Teppe, W. Desrat, S. Koohpayeh, L. Wu, N. P. Armitage,

A. Nateprov, E. Arushanov, Q. D. Gibson, R. J. Cava, D. van der Marel, B. A. Piot, C. Faugeras, G. Martinez, M. Potemski, and M. Orlita, Phys. Rev. Lett. **117**, 136401 (2016).

[38] Shin-Ming Huang, Su-Yang Xu, Ilya Belopolski, Chi-Cheng Lee, Guoqing Chang, BaoKai Wang, Nasser Alidoust, Guang Bian, Madhab Neupane, Chenglong Zhang, Shuang Jia, Arun Bansil, Hsin Lin, and M. Zahid Hasan, Nat. Commun. **6**, 7373 (2015).

[39] Hongming Weng, Chen Fang, Zhong Fang, B. Andrei Bernevig, and Xi Dai, Phys. Rev. X **5**, 011029 (2015).

[40] Su-Yang Xu, Ilya Belopolski, Nasser Alidoust, Madhab Neupane, Guang Bian, Chenglong Zhang, Raman Sankar, Guoqing Chang, Zhujun Yuan, Chi-Cheng Lee, Shin-Ming Huang, Hao Zheng, Jie Ma, Daniel S. Sanchez, BaoKai Wang, Arun Bansil, Fangcheng Chou, Pavel P. Shibayev, Hsin Lin, Shuang Jia, and M. Zahid Hasan, Science **347**, 294 (2015).

[41] B. Q. Lv, N. Xu, H. M. Weng, J. Z. Ma, P. Richard, X. C. Huang, L. X. Zhao, G. F. Chen, C. E. Matt, F. Bisti, V. N. Strocov, J. Mesot, Z. Fang, X. Dai, T. Qian, M. Shi, and H. Ding, Nat. Phys. **11**, 724 (2015).

[42] L. X. Yang, Z. K. Liu, Y. Sun, H. Peng, H. F. Yang, T. Zhang, B. Zhou, Y. Zhang, Y. F. Guo, M. Rahn, D. Prabhakaran, Z. Hussain, S.-K. Mo, C. Felser, B. Yan, and Y. L. Chen, Nat. Phys. **11**, 728 (2015).

[43] See Supplemental Material for the experimental details, the single-crystal growth, the fitting details, the DFT + DMFT calculations and the theoretical calculations of the LL spectrum and the optical selection rule.

[44] David C. Johnston, Adv. Phys. **59**, 803-1061 (2010).

[45] Pengcheng Dai, Jiangping Hu, and Elbio Dagotto, Nature Phys. **8**, 709-718 (2012).

[46] M. Tokunaga, I. Katakura, N. Katayama, and K. Ohgushi, J. Low Temp. Phys. **159**, 601605 (2011).

[47] C. Ma, H. X. Yang, H. F. Tian, H. L Shi, J. B. Lu, Z. W. Wang, L. J. Zeng, G. F. Chen, N. L. Wang, and J. Q. Li, Phys. Rev. B **79**, 060506(R) (2009).

[48] M. A. Tanatar, A. Kreyssig, S. Nandi, N. Ni, S. L. Bud'ko, P. C. Canfield, A. I. Goldman, and R. Prozorov, Phys. Rev. B **79**, 180508(R) (2009).

[49] Jiun-Haw Chu, James G. Analytis, David Press, Kristiaan De Greve, Thaddeus D. Ladd, Yoshihisa Yamamoto, and Ian R. Fisher, Phys. Rev. B **81**, 214502 (2010).

[50] S. Zapf, C. Stingl, K. W. Post, J. Maiwald, N. Bach, I. Pietsch, D. Neubauer, A. Lhle, C. Clauss, S. Jiang, H. S. Jeevan, D. N. Basov, P. Gegenwart, and M. Dressel, Phys. Rev. Lett. **113**, 227001 (2014).

[51] E. D. Palik, and J. K. Furdyna, Rep. Prog. Phys. **33**, 1193-1322 (1970).

[52] M. Orlita, Liang Z. Tan, M. Potemski, M. Sprinkle, C. Berger, W. A. de Heer, Steven G. Louie, and G. Martinez, Phys. Rev. Lett. **108**, 247401 (2012).

[53] C. Faugeras, M. Amado, P. Kossacki, M. Orlita, M. Sprinkle, C. Berger, W. A. de Heer, and M. Potemski, Phys. Rev. Lett. **103**, 186803 (2009).

[54] L. Boeri, M. Calandra, I. I. Mazin, O. V. Dolgov, and F. Mauri, Phys. Rev. B **82**, 020506(R) (2010).

[55] Sándor Bordács, Joseph G. Checkelsky, Hiroshi Murakawa, Harold Y. Hwang, and Yoshinori Tokura, Phys. Rev. Lett. **111**, 166403 (2013).

[56] M. L. Sadowski, G. Martinez, M. Potemski, C. Berger, and W. A. de Heer, Phys. Rev. Lett. **97**, 266405 (2006).

[57] Z. Jiang, E. A. Henriksen, L. C. Tung, Y.-J. Wang, M. E.

Schwartz, M. Y. Han, P. Kim, and H. L. Stormer, Phys. Rev. Lett. **98**, 197403 (2007).

[58] R. Y. Chen, Z. G. Chen, X.-Y. Song, J. A. Schneeloch, G. D. Gu, F. Wang, and N. L. Wang, Phys. Rev. Lett. **115**, 176404 (2015).

[59] Z. P. Yin, K. Haule, and G. Kotliar, Nat. Phys. **7**, 294-297 (2011).

[60] Z. P. Yin, K. Haule, and G. Kotliar, Nat. Mater. **10**, 932-935 (2011).

[61] Phillip E. C. Ashby, and J. P. Carbotte, Phys. Rev. B **87**, 245131 (2013).

[62] V. P. Gusynin, S. G. Sharapov and J. P. Carbotte, J. Phys.: Condens. Matter **19**, 026222 (2007).